ANS MC2015 - Joint International Conference on Mathematics and Computation (M&C), Supercomputing in Nuclear Applications (SNA) and the Monte Carlo (MC) Method · Nashville, Tennessee · April 19–23, 2015, on CD-ROM, American Nuclear Society, LaGrange Park, IL (2015)

PROTON-INDUCED GAIN IN A PORTABLE FARADAY CUP

Shaun Marshall and Blake Currier
Department of Physics
Worcester Polytechnic Institute
100 Institute Rd, Worcester, MA 01609

Andrew D Hodgdon, CHP
Radsim, LLC
584 Grove St, Newton, MA 02462
adhodgdon@radsim.org

ABSTRACT

A Portable Faraday Cup (PFC) is being designed to calibrate therapy-range proton accelerators (50 to 250 MeV). The PFC must be accurate to 1% and practical, hence vacuum-less and of low mass. Copper was chosen as the detector core, coated with a Kapton insulating film and silver ground. The Monte Carlo method (MCNP6 and Geant4) was used to simulate the radiation cascade and predict gain versus height (H), diameter (D) and insulator thickness (K). H and D were mostly functions of proton range; both are proportional to mass and inversely so to proton leakage, and thus decreases detector accuracy. Kapton functions to capture backscattered electrons, the function of the fields in a standard Faraday Cup. Greater K increases capture but increases secondary electron in-leakage. Determining optimal K was made difficult by the lack of low energy proton and electron cross-sections. A secondary electron model was programmed with the SDEF command for the MCNP model based on recently published cross-section approximations. This secondary electron source method was benchmarked against a series of experimental measurements of protons on copper and on water.

Key Words: Monte Carlo, Geant4, MCNP6, Faraday Cup, Proton Beam, Secondary Electron Emission

1 INTRODUCTION

In modern radiation therapy, protons have become an increasingly popular method of treating cancer near critical structures, with many dosimetric advantages of charged particle interactions [1,2]. A novel, portable, vacuumless Faraday Cup for detecting charged particles was designed to calibrate proton therapy facilities, in energies ranging from 50 to 250 MeV. The detector is constructed of a copper cylinder, coated with Kapton insulation and grounded with silver (CITE). Monte Carlo computational simulations in MCNP6 (CITE) and GEANT4 (CITE) were performed to evaluate radiation cascade effects and predict signal versus height, diameter and insulator thickness characteristics.

Preliminary results indicated that increasing the mass of the Faraday Cup's conductor reduced proton leakage but increased the system accuracy. While additional Kapton captures more primary

and secondary electrons, it also increases secondary electron leakage into the copper. Optimizing this Kapton thickness has been made difficult by the lack of low energy proton and electron cross-sections in current Monte Carlo based simulation programs (CITE). A comprehensive secondary electron evaluation of the Kapton was performed and benchmarked against a series of experimental measurements by J. Gordon et al [3].

In corroboration with the computational calculations, three prototype Faraday Cup devices were constructed by Pyramid Technical Consultants, Inc. (Waltham, Ma), each with a different thickness of Kapton. The units were tested in Germany to determine accuracy of the new design.

2 EXPERIMENTAL BACKGROUND

Limited empirical evidence of proton-beam dose was available before the gold/aluminum-oxide Faraday Cup emulations at the Los Alamos National Laboratory, which produced charged-particle beam current yields as a function of (at the time, the highest) beam energies from 5-24 MeV; it was found that secondary electron yield varied inversely with impinging proton beam energy, fitting an inverse-root curve (as predicted by Sternglass) with approximately 10% error. [4, 5]. This was later semi-empirically validated with similar models [6] and simulation using a constant-proportionality estimate of the secondary electron yield with the stopping power of protons in respective materials [7]; however, evidence exists which questions the validity of the latter approximation [8]. Though simulation techniques struggle to converge to comparable values for low beam energy scenarios, the findings establish a reasonable basis in setting the Faraday Cup depth to extend further than the material-specific range of the the particle. This removes the possibility of transmission-sputtering and second-surface electron emission occurences, providing the user with a more controlled ammeter measurement [4].

A unique approach to the Faraday Cup, a series of copper sheets separated by Kapton insulators, was tested in the Harvard Cyclotron Laboratory at a much higher energy. This “Multilayer" prototype provided empirical data to benchmark the applicability of separate hadronic interaction modules of Geant3.2.1. Each sheet of Kapton offers a mid-range, low-interaction field within which secondary electrons (or other stray charged particles) and their abandoned ion may remain bound to each other [9]. This novel approach of “trapping" the electrons which would not otherwise be impeded by the dense metal localizes the effects of Coulombic scattering and normalizes the measured total signal of the charged particles scattered per unit length and beam input; a gain differential of depth, independent of contributions of secondary electrons in the air. The role of the vacuum to constrain particle flux was transferred to a silver external grounding brace in the experiments carried out by the Heidelberg Institute of Technology in a recent development to incorporate portability in measuring device. Current efforts are directed at establishing proof-of-concept theoretically with simulated reproduction.

3 SIMULATION RESULTS

A variety of adaptations to the model were examined with both MCNP6 and Geant4 Monte Carlo software, the latter across a high-energy spectrum

3.1 MCNP6

MCNP version 6.1 with standard cross-section libraries was used to simulate gain. The Faraday Cup geometry is shown in Fig. 1. The height of the cylinder is fixed at 10 cm. The diameter is varied from 2 to 10 cm and the Kapton thickness is varied from 25 to 75 microns. The materials are standard copper, Kapton, silver and air at STP. The source is a 2 cm diameter proton beam at 250 MeV. This is the maximum expected energy. A suitable diameter for this energy will be suitable for lower energies. Physics was turned on for seven particles: neutrons, photons, electrons, protons, deuterons, tritons and alphas.

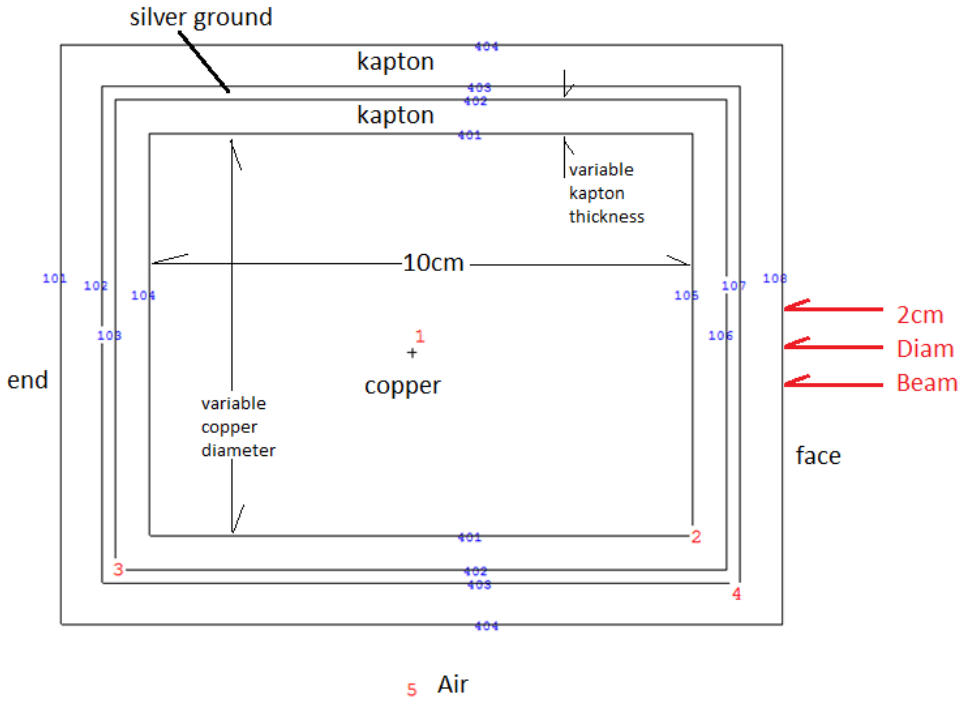

Figure 1. Geometry from side of horizontal copper cylinder

Gain was modeled simplistically by tallies of two charged particles (protons and electrons) crossing three surfaces (face, side and end). Gain is expressed in terms of elemental charge deposited in copper per beam proton, shown in eq. 1.

$$Gain = \frac{\sum Q_{particle \rightarrow Cu} - \sum Q_{particle \leftarrow Cu}}{\sum Q_{P+\ beam}} \tag{1}$$

MCNP6 distinguishes between two types of secondary electrons, those that are created by proton collisions, i.e., SE_h, (MCNP cannot track such electrons), and those that are generated by other particles (notably photons that are themselves secondary), i.e., $SE_{!h}$. The following assumptions were made in this model:

- For the selection of a good copper diameter the SE_h are not important (untested)
- Protons and electrons are the only contributors to gain (valid within range of 2E-4)
- The choice of copper diameter has little effect on the detailed behavior of $SE_{!h}$ electrons in Kapton (i.e., capture causing mirror charge in copper). This means that the location and energy of electrons captured in the kapton do not have to be tallied to get valid answer for the copper diameter (untested)

The detector is to be a beam proton counter. The perfect detector will yield a gain of unity, seen in eq. 2.

$$Error = (Gain - 1) \cdot 100\% \tag{2}$$

3.2 Geant4

Geant4 is an object-oriented C++ toolkit for developing applications which simulate the passage of particles through matter. Libraries of cross-section tables, elemental/molecular properties, and pre-defined stochastic physics processes allow for rapid, intuitive invocation of necessary system setup commands. Once initialized, “Manager" modules cooperate to organize and accumulate dynamic information which is organized in the following chronology:

1. The **DetectorConstruction** class is called to verify, store and lock the predefined geometry.
2. The **G4UIManager** initializes upon successful compilation and execution of the *main()* routine. If a visualizer is selected, **G4VisManager** is also invoked.
3. The user issues the command to execute a macro file of *runs*; each run is characterized by the defined beam particle type, the beam energy, and the number of *events*, or number of such isolated simulations. If multithreading is available, **G4RunManager** allocates the events to the available worker threads on a rolling basis.
4. For each event, the simulation of the *primary* (beam) particle proceeds, constructing a new *track*, or well-defined trajectory for every particle not at rest.
5. The behavior of every track is determined dynamically, with each *step*, or stochastically occuring physical process (collisions, absorbtions, etc) of the particle in some medium.

3.2.1 UserAction methods

A useful feature of Geant4 is the ability to create user-defined actions (methods) throughout each module, which allows for a very fine-tuned analysis throughout the entire simulation. The following summarizes the custom details and methods for this application

Table I. Geant4 Simulation Cylindrical Construction

Volume	Radius (mm)	Height (mm)
Copper	30	100
	Model	Thickness (μm)
Kapton1	S59	59
	S100	100
	S200	200
Silver	+Ag/KA	12
Kapton2	+Ag/KA	62

- **DetectorConstruction.cc:** A copper cylinder of radius 3 cm and height 10 cm is covered in Kapton film of varying thickenesses: 59 μm, 100 μm and 200 μm. The film thickness is iterated by a function which is called before the command macro is examined. The top face of the copper lies in the $z = 0$ plane, with the beam approach the system from beneath.

- **SteppingAction.cc:** [For every step,] immediately checks if the step is the finale of a track. If so, the particle's vertex (original position) and destination volume and coordinates are found, and a charge signal calculation occurs. Entering/Leaving the copper gives a net signal of $\pm q$ where q is the charge of the particle. Entering/Leaving Kapton gives a relative proportionality of

$$s_{q \rightleftharpoons KA} = \pm q \times \max\left[r_{\%}, z_{\%}\right], \tag{3}$$

  where $r_{\%}$ is the percent distance away from the copper radially and $z_{\%}$ is the percent distance away laterally. The signals are grouped and saved by a unique eventID number.

- **EventAction.cc:** At the end of each event, the signals are tallied, grouped, and saved by a unique runID number.

- **RunAction.cc:** At the end of each run, the average and standard deviation of the signals are acquired.

3.2.2 Experimental parameters

Table I summarizes the detector geometry of each run. The order of logical volume layers starting from the innermost are 1) the copper cylinder, 2) the Kapton1 film, 3) the silver paint layer, and 4) the Kapton2 film. Constructing cylindrical "layers" is as straightforward as defining a cylinder within another's logical volume. Data were acquired as a function of impinging proton energy using the 50-250 MeV range as used in the HIT experiment. The Kapton1 thickness optimization was applied to this model both with and without the silver and secondary Kapton (*+Ag/KA*).

4 RESULTS

(LATER: intro info here)

4.1 MCNP6 Simulation

Fig. 2 shows the variation of error with copper diameter and method. Two methods are compared, SRIM (reference) and MCNP6. A diameter of 6cm seems reasonable.

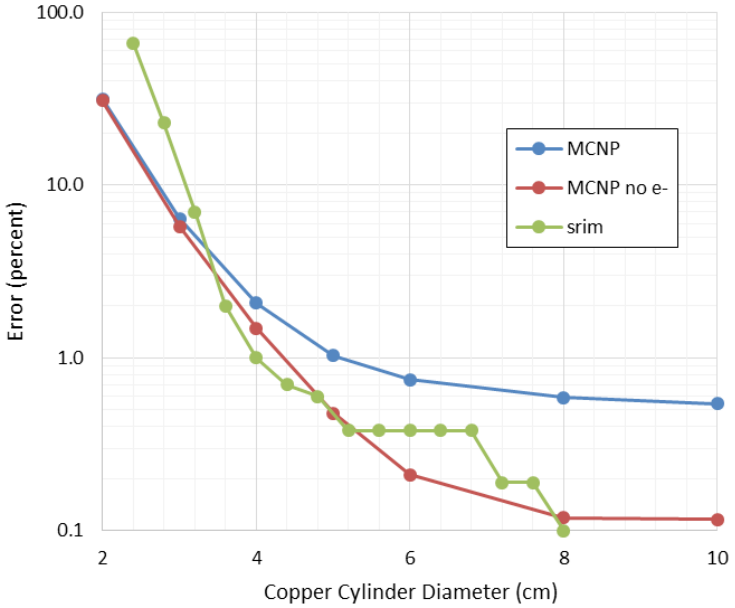

Figure 2. Signal Error vs Diameter and Simulation Method

The same calculation was repeated with proton tallies alone, i.e., without any secondary electrons. This shows that if electrons had been completely ignored, the MCNP6 results would have been similar to the SRIM model and a diameter of 8 cm would have seemed reasonable.

The distribution of proton collisions from 50 beam protons is in Fig. 3. The distribution of 6 other particles (born of 50 Protons) is in Fig. 4; neutrons go everywhere. The distribution of electrons (just type $SE_{!h}$) is similar to photons. Table II shows the boundary crossings of neutral particles. In the problem there are about two neutral particle boundary crossings per beam proton.

Table III shows the breakdown of gain from various charged particles for given directions and copper surfaces. This assumes 250 MeV Proton Beam, 6cm Copper Diameter and 50 microns

kapton. The effect of secondary electrons produced directly by proton collisions (SD_h) is not included.

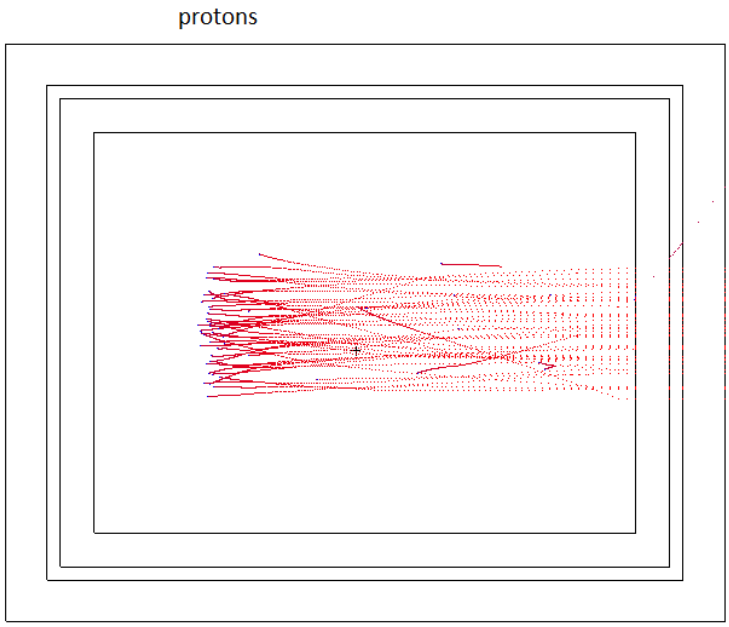

Figure 3. Distribution of 50 Protons of Energy 250 MeV using MCNP6. Note the singular backscatter.

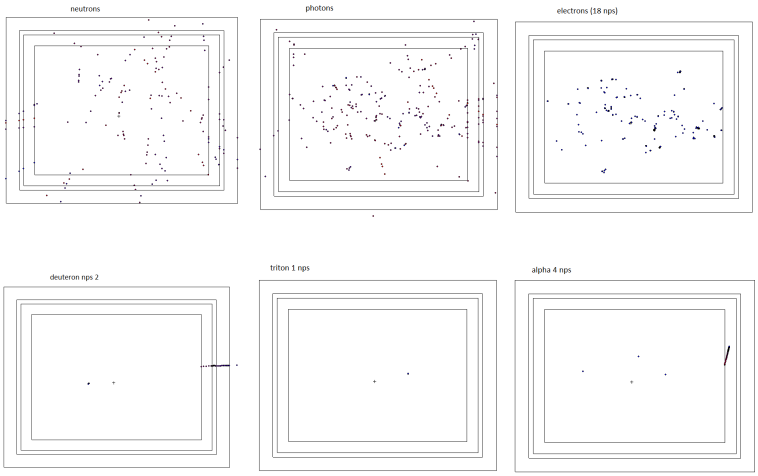

Figure 4. Distribution of six other particles

It is worth examining the behavior of the model. Kapton thickness (25, 50 and 75 microns) seems to make no difference in gain. Neither do the inclusion of tallies for deuterons, tritons and alphas, although the MCNP output file notes the absence of production cross-sections for these

particles*. All of the figures and tables below were for the case of 6cm diameter, 50 microns of kapton and 50 beam protons of energy 250 MeV.

Table II. Charges Crossing Copper Surfaces (fraction per proton source) assuming 250 MeV Proton Beam, 6 cm Copper diameter, 50 microns of Kapton, and no SE_h

Particle	tally	face	cylinder	end	total
n	in	0.000 65	0.000 44	0.106 92	0.108 01
	out	0.148 74	0.678 67	0.000 07	0.827 47
γ	in	0.000 38	0.000 70	0.000 11	0.001 19
	out	0.176 03	0.650 51	0.078 12	0.904 66

Table III. Charges Crossing Copper Surfaces (fraction per proton source) assuming 250 MeV Proton Beam, 6 cm Copper diameter, 50 microns of Kapton, and no SE_h

Particle	tally	face	cylinder	end	total
P+	in	0.999 97	0.000 00	0.000 00	0.999 97
	out	0.000 55	0.001 23	0.000 23	0.002 01
	total	0.999 41	0.001 23	0.000 23	0.997 96
E (no SE_h)	in	0.000 31	0.000 87	0.000 10	0.001 28
	out	0.001 49	0.004 50	0.000 51	0.006 50
	total	0.001 19	0.003 62	0.000 42	0.005 23
d	in	0.000 03	0.000 00	0.000 00	0.000 03
	out	0.000 07	0.000 06	0.000 02	0.000 15
	total	0.000 04	0.000 06	0.000 02	0.000 12
t	in	0.000 02	0.000 00	0.000 00	0.000 02
	out	0.000 03	0.000 06	0.000 02	0.000 03
	total	0.000 01	0.000 06	0.000 02	0.000 01
a	in	0.000 03	0.000 00	0.000 00	0.000 03
	out	0.000 03	0.000 00	0.000 00	0.000 03
	total	0.000 00	0.000 00	0.000 00	0.000 00
Signal	in	0.999 74	0.000 87	0.000 10	1.001 24
	out	0.000 82	0.003 20	0.000 26	0.008 51
	total	0.998 23	0.004 85	0.000 65	0.992 73

4.2 Geant4 Simulation

Signal gain is defined in eq. 1. Charges entering and leaving the primary Kapton film covering the copper are subject to the linear proportion behavior defined in Eq. 3. Table IV shows a sample

*The absence of ion production XS noted in the MCNP output file vs the presence of ions in the run needs to be checked out.

output of each model in both air and vaccuum, the latter to remove oversaturation of beta emissions from the air due to delta-ray production (LATER: citation needed).

Table IV. Predicted Gain from High-Energy Protons using Geant4

Model	Energy (MeV)	(-Ag/KA)	(-Ag/KA) *in vacuo*	(+Ag/KA)	(+Ag/KA) *in vacuo*
S59	70.03	0.953 588	0.974 846	0.963 133	0.963 262
	100.46	0.967 417	0.984 694	0.970 072	0.970 867
	130.52	0.975 593	0.990 117	0.974 286	0.976 064
	160.09	0.981 094	0.994 044	0.978 484	0.980 236
	190.48	0.985 111	0.996 718	0.981 775	0.983 519
	221.06	0.988 151	0.999 012	0.984 790	0.986 344
	250.00	0.990 298	1.000 260	0.986 376	0.987 953
S100	70.03	0.953 827	0.974 725	0.962 994	0.963 440
	100.46	0.966 795	0.984 533	0.970 114	0.970 319
	130.52	0.975 725	0.990 464	0.974 399	0.980 993
	160.09	0.981 055	0.994 167	0.978 401	0.976 085
	190.48	0.985 189	0.996 801	0.981 909	0.980 045
	221.06	0.988 149	0.999 164	0.984 451	0.983 287
	250.00	0.990 324	1.000 160	0.986 188	0.988 118
S200	70.03	0.954 372	0.974 735	0.962 984	0.963 351
	100.46	0.966 915	0.984 373	0.970 077	0.971 036
	130.52	0.975 377	0.990 337	0.974 646	0.976 159
	160.09	0.980 998	0.994 016	0.978 510	0.980 092
	190.48	0.985 217	0.996 776	0.981 840	0.983 659
	221.06	0.988 312	0.999 045	0.984 644	0.986 081
	250.00	0.990 213	0.999 940	0.986 601	0.988 010

Fig. 5 depicts the tracks of particles given the simulation of 50 250 MeV protons entering the S59 model. The track color corresponds to particle charge, red for negative, blue for positive, and green neutral. As observed in the MCNP6 simulation, neutrons are scattered everywhere; for the most part, electrons created in the Faraday Cup do not travel far, as expected given their low-energy production and high stopping-power in copper. Fig. 6 compares the Geant4 variants with the measured gains of homologous Faraday Cups at HIT.

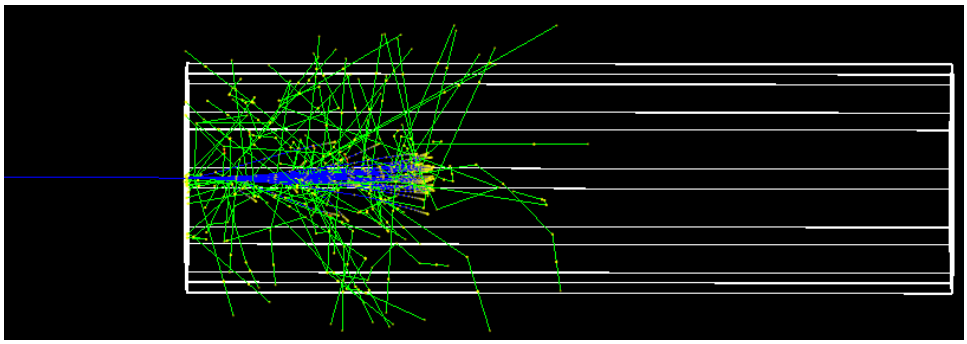

Figure 5. Distribution of 50 Protons of Energy 250 MeV using Geant4.

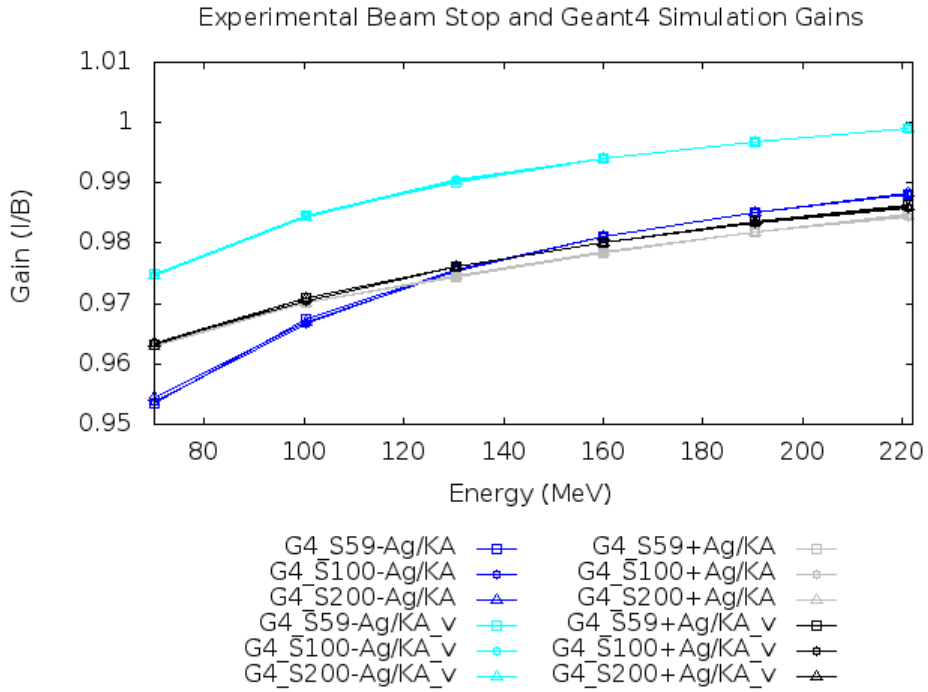

Figure 6. Comparison of Geant4 output and HIT measurement. Generated with Gnuplot.

5 DISCUSSION

It is known that MCNP does not track electrons secondary to protons. Therefore, there are delta rays and secondary electrons from protons that have not been accounted for. This means that the error is greater than has been portrayed and needs further investigation because it is shown in Fig. 2 that electron production (just the $SE_{!h}$) is impacted by the diameter on the choice of diameter.

The electrons that are included are those that are secondary to the particle cascade subsequent to protons. For example, there are electrons secondary to photons that come from neutrons that come from protons. Table II shows that there are almost 2 neutral particles crossing the Faraday Cup boundary per beam proton. It is important to note that the addition of deuterons, tritons and alphas

changes the gain by -0.0002[†], and that there were no proton creation cross-sections for Ag-107, so it was substituted for Ag-109 which makes up about 2/3 of the silver.

In pursuit of the optimization of this portable Faraday Cup, we considered many variants of applicable theoretical models to corroborate with available experimental data. Fig. 6 depicts a very convincing similarity in behavior between the HIT beam stop measurements and the simulation of the copper Faraday Cup in air without the *no* silver/Kapton layer. Shown by the thin separation between plots and occasional crossovers, there are no readily identifiable trends of increasing Kapton thickness (LATER: ONE LAST CONTROL RUN OF PURE COPPER). Replacing the air with a vacuum outermost layer increases the overall positive charge of the detector (CITE: delta ray info), however this change is quite small ($\ll 1\%$), and is therefore likely more indicitive of negligible difference [4].

6 CONCLUSIONS

7 ACKNOWLEDGMENTS

We would like to express our sincerest gratitude to Paul Romano and Tom Sutton, who provided the template for this paper.

8 REFERENCES

[1] W. Newhauser, N. Koch, S. Hummel, M. Ziegler, and U. Titt, "Monte Carlo simulations of a nozzle for the treatment of ocular tumours with high-energy proton beams," *Physics in Medicine and Biology*, **50**, pp. 5229–5249 (2005).

[2] J. M. Ryckman, "Using MCNPX to Calculate Primary and Secondary Done in Proton Therapy," *Georgia Institute of Technology* (2011), (Master's thesis).

[3] J. Gordon and L. Magallanes, "Evaluation of Current Measuring Beam Stop," 2014, Proprietary Calculations.

[4] J. E. Borovsky, D. J. McComas, and B. L. Barraclough, "The Secondary-Electron Yield Measured for 5-24 MeV Protons on Aluminum-Oxide and Gold Targets," *Nuclear Instruments and Methods in Physics B*, **30**, pp. 191–195 (1988).

[5] E. Sternglass, "Theory of Secondary Electron Emission by High-Speed Ions," *Physical Review*, **108**, pp. 1 (1957).

[6] C. Castaneda, L. McGarry, C. Cahill, and T. Essert, "Secondary electron yields from the bombardment of Al2O3 by protons, deuterons, alpha-particles and positively charged hydrogen molecules at energies in the range of 10 to 80 MeV," *Nuclear Instruments and Methods in Physics Research B*, **129**, pp. 199–202 (1997).

[7] D. Kramer, "Design and Implementation of a Detector for High Flux Mixed Radiation Yields," *Technical University of Liberec* (2008), (Doctoral dissertation).

[†] See mc-ptc-11-3.0-f for effect of deuterons, tritons, and alphas.

[8] A. Dubus et al., "Experimental and theoretical study of the ratio between the electron emission yield and the electronic stopping power for protons incident on thin carbon foils," *Nuclear Instruments and Methods in Physics Research B*, **193**, pp. 621–625 (2002).

[9] B. Gottschalk, R. Platais, and H. Paganetti, "Nuclear interactions of 160 MeV protons stopping in copper: A test of Monte Carlo nuclear models," *Medical Physics*, **26**, pp. 2597 (1999).

APPENDIX A EXPERIMENTALS RESULTS AT HIT [3]

Table V. Measured Gain from HIT Beam Stops

Energy (MeV)	S59	S100	S200
70.03	0.9750	0.9385	0.9350
100.46	0.9850	0.9500	0.9475
130.52	0.9925	0.9580	0.9525
160.09	1.0000	0.9635	0.9590
190.48	1.0075	0.9715	0.9650
221.06	1.0125	0.9800	0.9770